Stochastic Chaos in a Class or Fokker-Planck Equations

Mark M. Millonas and Linda E. Reichl
Department of Physics and Center for Statistical Mechanics & Complex Systems, University of Texas at Austin, Austin, Texas 78712
(Received 8 November 1991)

We show that a large class of Fokker-Planck equations, like the Schrödinger equation, can exhibit a transition in their spectral statistics as a coupling parameter is varied. We assert that this transition is connected to the transition to nonintegrability in a particular set of Hamilton's equations. In the case of the Schrödinger equation, this transition is known to be a fingerprint of the underlying classical dynamics. However, the Hamilton's equations describing the transition in the Fokker-Planck spectrum have no direct physical relation to the underlying dynamics of the Fokker-Planck equation, and consequently have no such simple physical interpretation.

PACS numbers: 05.40.+j, 02.50.+s, 05.45.+b

The manifestations of chaos in a particular Fokker-Planck equation with time-dependent coefficients has been studied previously [1], where it was shown that the Floquet spectrum for that system exhibited a transition in its statistical properties. In this paper we show that not only can a whole class of Fokker-Planck equations with time-independent coefficients exhibit such transitions, but also how this transition can be related to the dynamical properties of certain Hamiltonian equations of motion. Such a relation, in addition to providing a framework for understanding and predicting such transitions, also provides a whole new set of concepts and techniques which have not previously been applied to stochastic processes, but which have proven quite useful in attempts to understand the quantum mechanical manifestations of chaos.

In this paper we will be concerned with diffusion processes on $\Re^n$ described by the set of coupled stochastic differential equations

$$dq^i(t) = -\partial^i\Phi(\mathbf{q})dt + \sqrt{g}\,dW^i(t), \quad i=1,\ldots,n, \tag{1}$$

where $\Phi(\mathbf{q})$ is a potential bounded from below, the $W^i(t)$ are uncorrelated Wiener processes, and g is a diffusion coefficient [2]. [Note that Eq. (1) describes a purely classical diffusion process, and leads to a purely classical Fokker-Planck equation (2). Although not the only possible physical basis for this equation, one might think of (1) as a mechanical system with potential proportional to Φ, subject to very strong friction in a fluctuating environment.] In this case the evolution of the probability density $\rho(\mathbf{q},t)$ on $\Re^n$ is described by the Fokker-Planck equation [3]

$$\partial_t\rho = \frac{g}{2}\Delta\rho + \nabla\cdot(\rho\nabla\Phi). \tag{2}$$

Using the time separation ansatz $\rho(\mathbf{q},t)=\rho(\mathbf{q})e^{-\lambda t/g}$, we can write Eq. (2) as an eigenvalue equation $\mathcal{L}\rho_\lambda(\mathbf{q}) = -\lambda\rho_\lambda(\mathbf{q})$, where $\mathcal{L} = \frac{1}{2}g^2\Delta + g\nabla^2\Phi + g\nabla\Phi\cdot\nabla$. After the change of basis $\rho(\mathbf{q}) = e^{-\Phi/g}\Psi(\mathbf{q})$ we obtain

$$\mathcal{H}\Psi_\lambda(\mathbf{q}) = \lambda\Psi_\lambda(\mathbf{q}), \tag{3}$$

where $\mathcal{H} = -e^{\Phi/g}\mathcal{L}e^{-\Phi/g} = -\frac{1}{2}g^2\Delta + \hat{\Phi}(\mathbf{q})$ is a Hermitian Schrödinger-type operator with the transformed potential $\hat{\Phi} = \frac{1}{2}(\nabla\Phi)^2 - \frac{1}{2}g\nabla^2\Phi$. The problem of solving Eq. (2) has been reduced to the problem defined by Eq. (3).

For small g [4] the WKB solutions of Eq. (3) are given by

$$\Psi_\lambda(\mathbf{q}) = \sum_a c_a|\nabla S_a|^{-1/2}\exp\left[\frac{i}{g}S_a(\mathbf{q},\lambda)\right], \tag{4}$$

where the $S_a(\mathbf{q},\lambda)$ are the solutions of the Hamilton-Jacobi equation $\frac{1}{2}(\nabla S_a)^2 + \hat{\Phi} = \lambda$. The solutions of this equation are given by the integrals $S_a(\mathbf{q},\lambda) = \int^{\mathbf{q}}\mathbf{p}_a\cdot d\mathbf{q}$ where the integration is along the classical trajectories of Hamilton's equations of motion [5]

$$\dot{\mathbf{p}} = -\frac{\partial H}{\partial \mathbf{q}}, \quad \dot{\mathbf{q}} = \frac{\partial H}{\partial \mathbf{p}}, \tag{5}$$

with

$$H(\mathbf{p},\mathbf{q}) = \tfrac{1}{2}\mathbf{p}^2 + \hat{\Phi}(\mathbf{q}). \tag{6}$$

The time-reversal symmetry of Eqs. (5) with Hamiltonian (6) insures that the eigenfunction (4) are real since the solutions of the Hamilton-Jacobi equation will come in pairs $\pm S_a$. The dynamics of (5) determine the solution of (3) through (4), and the solutions of (2) are given by

$$\rho_\lambda(\mathbf{q},t) = \exp\left[-\frac{\Phi+\lambda t}{g}\right]\Psi_\lambda(\mathbf{q}). \tag{7}$$

Thus the properties of the Fokker-Planck equation (2) are connected to the dynamics of the system with Hamiltonian (6) in a manner somewhat analogous to the relation of a quantum mechanical system to its classical counterpart.

One question we might ask is how the behavior of (2) is affected by the degree of chaos in the equations of motion (6). Such effects, in the quantum mechanical case [(5) affecting (3)], are often referred to as *quantum chaos*, which is usually defined as the characteristics of quantum systems whose classical analogs exhibit chaos.

The statistical properties of the eigenvalues of such systems are such characteristics, and the level spacing distribution $P(S)$, giving the probability of level separation S (measured in units of the local mean spacing), provides one such statistical property. Berry and Tabor [6] have shown that nearly all quantum systems whose classical analogs are integrable will have a Poisson level spacing distribution $P(S)=\exp(-S)$, indicating the statistical independence of neighboring energy levels. On the other hand, it is now understood that the eigenvalues of systems whose classical analogs are chaotic exhibit level repulsion. That is, $P(S)\to 0$ as $S\to 0$ [7]. It is expected that systems with time-reversal symmetry whose classical analogs are globally chaotic will have a Wigner level spacing distribution, $P(S)=(\pi S/2)\exp(-\pi S^2/4)$, indicating a linear level repulsion as $S\to 0$ [8]. Since the eigenvalues of the Fokker-Planck operator $\mathcal{L}$ with potential Φ are the negative of the eigenvalues of a Hamiltonian $\mathcal{H}$, with potential $\hat{\Phi}$, the spectral statistics of the Fokker-Planck equation (2) would then be expected to provide a signature of the dynamics of the equations of motion (5).

Stochastic chaos can then be defined, at least for the case of diffusion in a time-independent potential, as *the properties of stochastic systems described by Eq. (2) when the equations of motion (5) exhibit chaos.* In particular, given a family of potentials $\hat{\Phi}_\epsilon$ where the dynamics of (5) varies from globally integrable to globally chaotic as ϵ is increased, we would expect the spectral spacing distribution of the λ's to exhibit a corresponding transition from Poisson to Wigner level spacing statistics.

An entirely separate problem is the question of the direct physical relevance of the dynamics of (5) to the underlying microscopic dynamics as described by (1). One thing is clear: Chaos in (5) is emphatically *not* related to chaos in the dynamics generated by (1) with $g=0$, that is, $\dot{\mathbf{q}}=-\nabla\Phi(\mathbf{q})$. When there is no noise the individual trajectories just follow the gradient of the potential along the route of steepest descent stopping at any local minimum in Φ, so what would normally be considered the underlying microscopic dynamics is trivial, and never chaotic. In addition, it is easy to show directly from (1) that the behavior of the expectation of $\hat{\mathbf{q}}$ obeys the same equation $E\{\dot{\hat{\mathbf{q}}}\}=-\nabla\Phi$. Thus, there is no simple physical relationship between the dynamics of (5) and the dynamics of (1). However, a deeper analysis shows that Eqs. (5) are the imaginary-time equations of motion for the most probable trajectories. A discussion of this result will appear elsewhere.

As an illustration of these ideas, we studied a family of two-dimensional Fokker-Planck equations with potentials

$$\Phi_\epsilon(x,y)=2x^4+\tfrac{3}{5}y^4+\epsilon xy(x-y)^2. \tag{8}$$

The form of the potential was chosen for convenience only. The system needed to be at least two dimensional in order to observe chaos in Eqs. (5). When $\epsilon=0$ the system is completely integrable, since it decouples into two one-dimensional systems. $\hat{\Phi}_\epsilon$ takes the form

$$\hat{\Phi}_\epsilon=(32+\tfrac{1}{2}\epsilon^2)x^6+(\tfrac{72}{25}+\tfrac{1}{2}\epsilon^2)y^6-g(12x^2+\tfrac{18}{5}y^2)$$
$$+\epsilon\{(24-4\epsilon)x^5y+(\tfrac{36}{5}-4\epsilon)xy^5-(32-\tfrac{31}{2}\epsilon)x^4y^2-(\tfrac{48}{5}-\tfrac{31}{2}\epsilon)x^2y^4+(\tfrac{52}{5}-24\epsilon)x^3y^3-2g(x^2+y^2-3xy)\}. \tag{9}$$

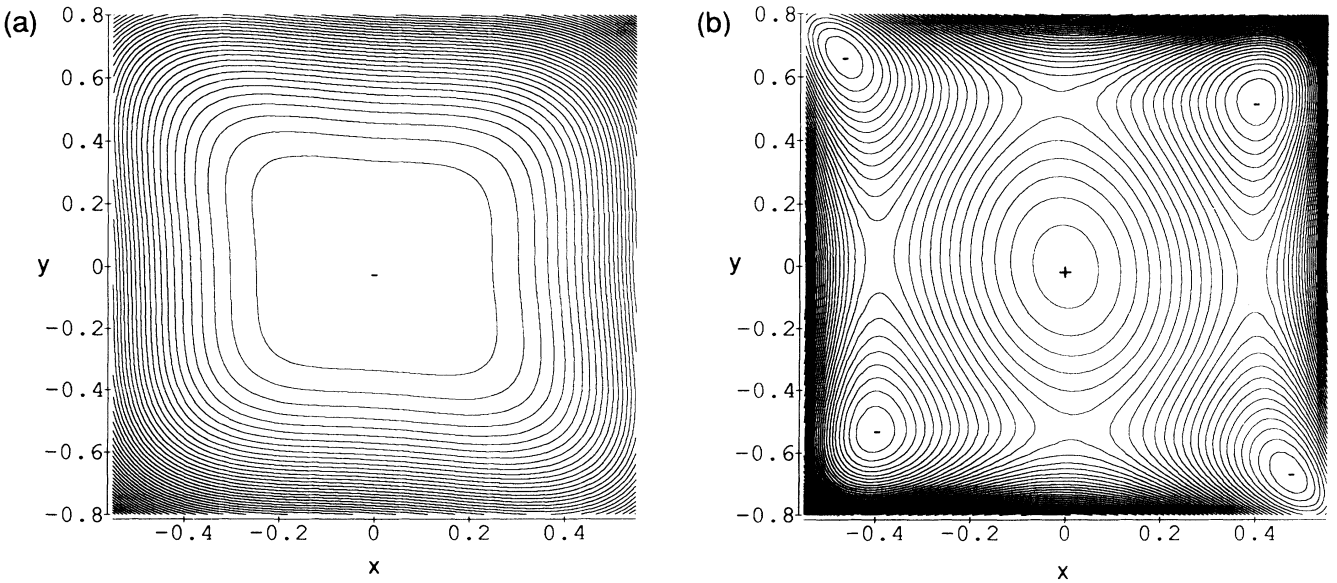

FIG. 1. Contour plots of the basins of (a) the physical potential Φ_ϵ and (b) the noise-dependent transformed potential $\hat{\Phi}_\epsilon$ for $\epsilon=0.10$ and $g=0.2$, which corresponds to case (d) in Fig. 2. The + and − signs mark the location of the local maxima and minima, respectively.

In Fig. 1 we compare contour plots of the physical potential Φ_ϵ to the noise-dependent transformed potential $\hat{\Phi}_\epsilon$.

The numerical scheme we used was essentially identical to the one used in [9]. The eigenvalues of $\mathcal{L}$ were calculated by expanding $\mathcal{H}$ in a harmonic oscillator basis and truncating the matrix at a suitably large size. The presence of only even order polynomial terms preserves parity, and enables us to calculate the eigenvalues for the even and odd parity matrices separately, markedly reducing the computation time. The eigenvalues of the truncated matrices were then obtained numerically. The unfolded level spacings are calculated by normalizing to local mean spacing unity via the formula $S_i = (\lambda_{i+1} - \lambda_i) \times \rho(\lambda_i)$, where $\rho(\lambda)$ is the smoothed level density. The unfolded level spacings of each parity matrix must be calculated separately. They can then be combined into one large ensemble to calculate $P(S)$. We were able to calculate 450–500 accurate eigenvalues for each parity matrix of rough dimension 2600.

The form of $\Phi(x,y)$ was chosen so that the dynamics and degree of chaos in Eqs. (5) would be nearly the same on differing λ (energy) surfaces in the range of eigenvalues considered. We set $g = 0.2$ in each case, and the reliable eigenvalues were in the range $0 \leq \lambda \leq 50$. This encompassed the first 900–1000 levels. Figure 2 illustrates the transition (as ϵ is varied) in the level spacing statistics

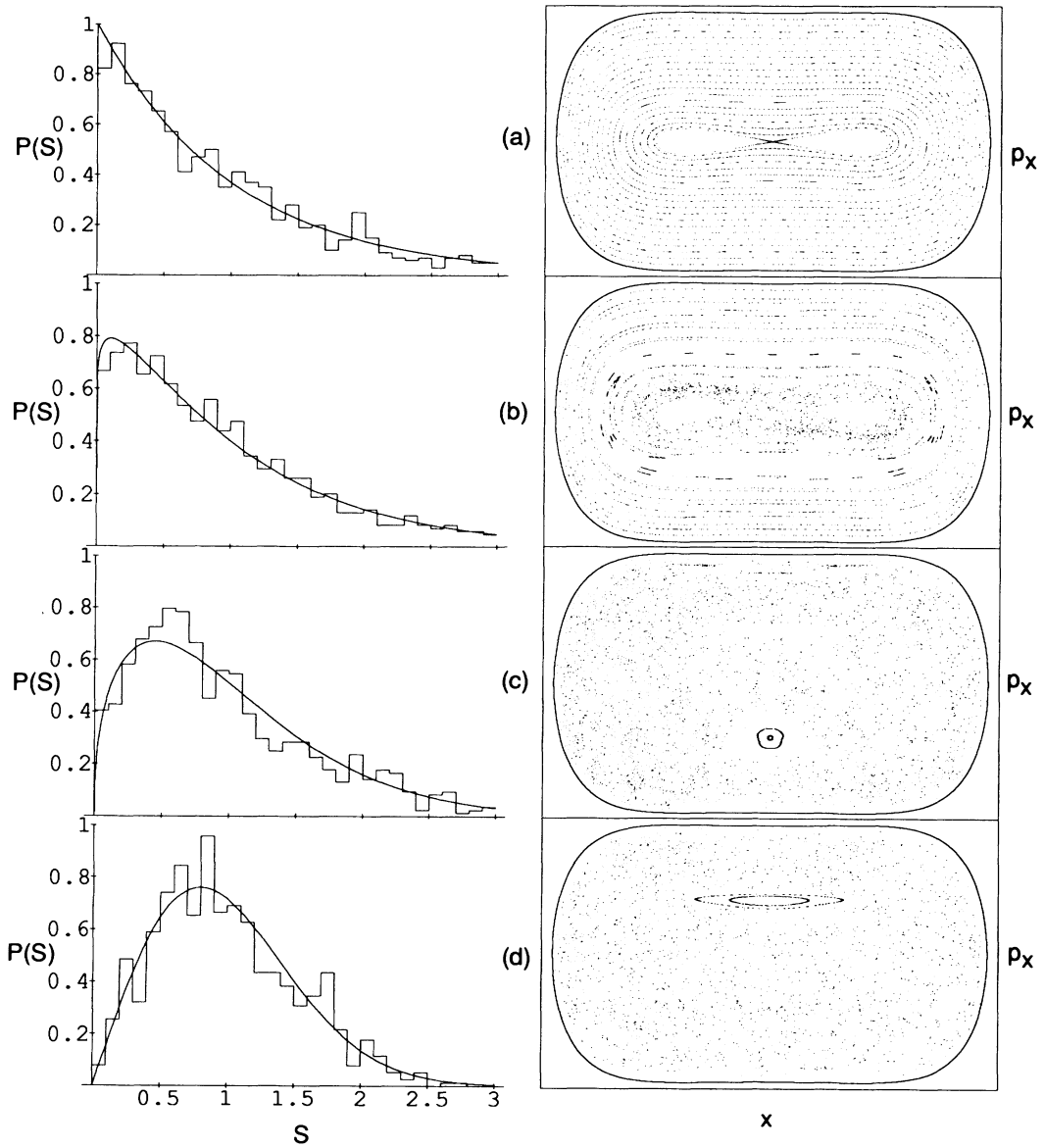

FIG. 2. Level spacing distributions $P(S)$ and the corresponding Poincaré cross sections of the model system with $g = 0.2$ for (a) $\epsilon = 0.0$, (b) $\epsilon = 0.005$, (c) $\epsilon = 0.04$, and (d) $\epsilon = 0.10$. The cross sections are taken for $(y = 0, p_y > 0)$, where $\lambda = 25$. The solid outlines represent the outermost boundary of the $\lambda = 25$ energy surface as projected onto the (x, p_x) plane.

of the Fokker-Planck operator as the dynamics of Eqs. (5) changes from completely integrable ($\epsilon=0$) to almost globally chaotic ($\epsilon=0.14$).

The formal relationship between the Fokker-Planck equation and the Schrödinger equation has been utilized before [3], but never in this way. It has often been pointed out that there is a deep analogy between quantum fluctuations and thermal fluctuations [10]. It now appears that there is also a deep analogy between quantum dynamics and stochastic dynamics through their relationship to the properties of certain conservative dynamical systems. This connection, once made, opens up the study of stochastic processes to a whole range of new tools and concepts applicable to nonlinear systems. For instance, what relationship does the Komogorov entropy or Lyapunov exponent [11] of (5) bear to the properties of the Fokker-Planck equation (2), and what does a nonlinear resonance in (5) correspond to in (2)? This is an area for further, possibly fruitful study.

Both of the authors wish to thank the Welch Foundation of Texas for partial support of this work through Grant No. F-1051.

[1] L. E. Reichl, Zhong-Ying Chen, and M. M. Millonas, Phys. Rev. Lett. **63**, 2013 (1989); Phys. Rev. A **41**, 1874 (1990).

[2] L. Arnold, *Stochastic Differential Equations: Theory and Applications* (Wiley, New York, 1974); W. Horsthemke and R. Lefever, *Noise-Induced Transitions* (Springer-Verlag, Berlin, 1984).

[3] H. Risken, *The Fokker-Planck Equation* (Springer-Verlag, Berlin, 1984).

[4] See any good quantum mechanics text, for instance, K. Gottfried, *Quantum Mechanics* (Benjamin, New York, 1966).

[5] H. Goldstein, *Classical Mechanics* (Addison-Wesley, Reading, MA, 1980).

[6] M. V. Berry and M. Tabor, Proc. R. Soc. London A **356**, 375 (1977).

[7] M. V. Berry, in *The Wave-Particle Dualism,* edited by S. Diner *et al.* (Reidel, Dordrecht, 1984); in *Proceedings of the International Conference of Cuernavaca, 1986,* edited by T. H. Seligman and H. Nishioka, Lecture Notes in Physics Vol. 263 (Springer-Verlag, Berlin, 1986); M. C. Gutzwiller, *Chaos in Classical and Quantum Mechanics* (Springer-Verlag, Berlin, 1990); L. E. Reichl, *The Transition to Chaos in Conservative Classical Systems: Quantum Manifestations* (Springer-Verlag, Berlin, 1992).

[8] E. P. Wigner, SIAM Rev. **9**, 1 (1967).

[9] T. H. Seligman, J. J. M. Verbaarschot, and M. R. Zirnbauer, J. Phys. A **18**, 2751–2770 (1985).

[10] G. Parisi, *Statistical Field Theory* (Addison-Wesley, Reading, MA, 1988); S. H. Shenker, in *Recent Advances in Field Theory and Statistical Mechanics,* edited by J. B. Zuber and R. Stora (North-Holland, Amsterdam, 1984).

[11] Zhong-Ying Chen, Phys. Rev. A **42**, 5837 (1990).

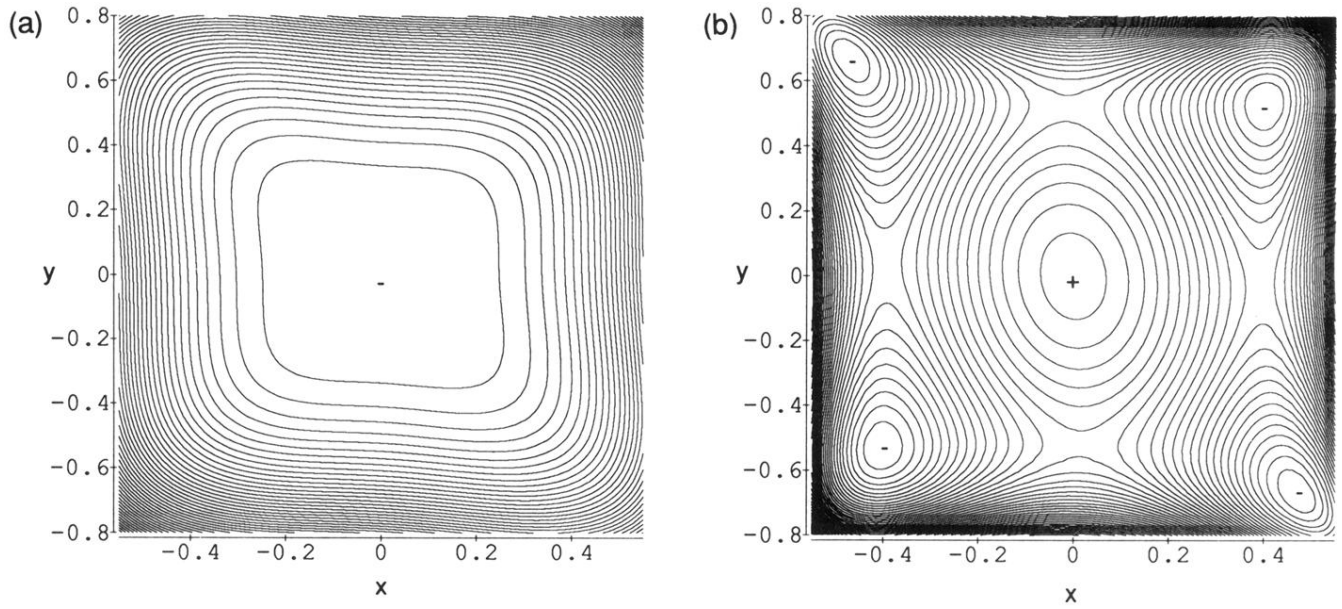

FIG. 1. Contour plots of the basins of (a) the physical potential Φ_ϵ and (b) the noise-dependent transformed potential $\hat{\Phi}_\epsilon$ for $\epsilon = 0.10$ and $g = 0.2$, which corresponds to case (d) in Fig. 2. The + and − signs mark the location of the local maxima and minima, respectively.

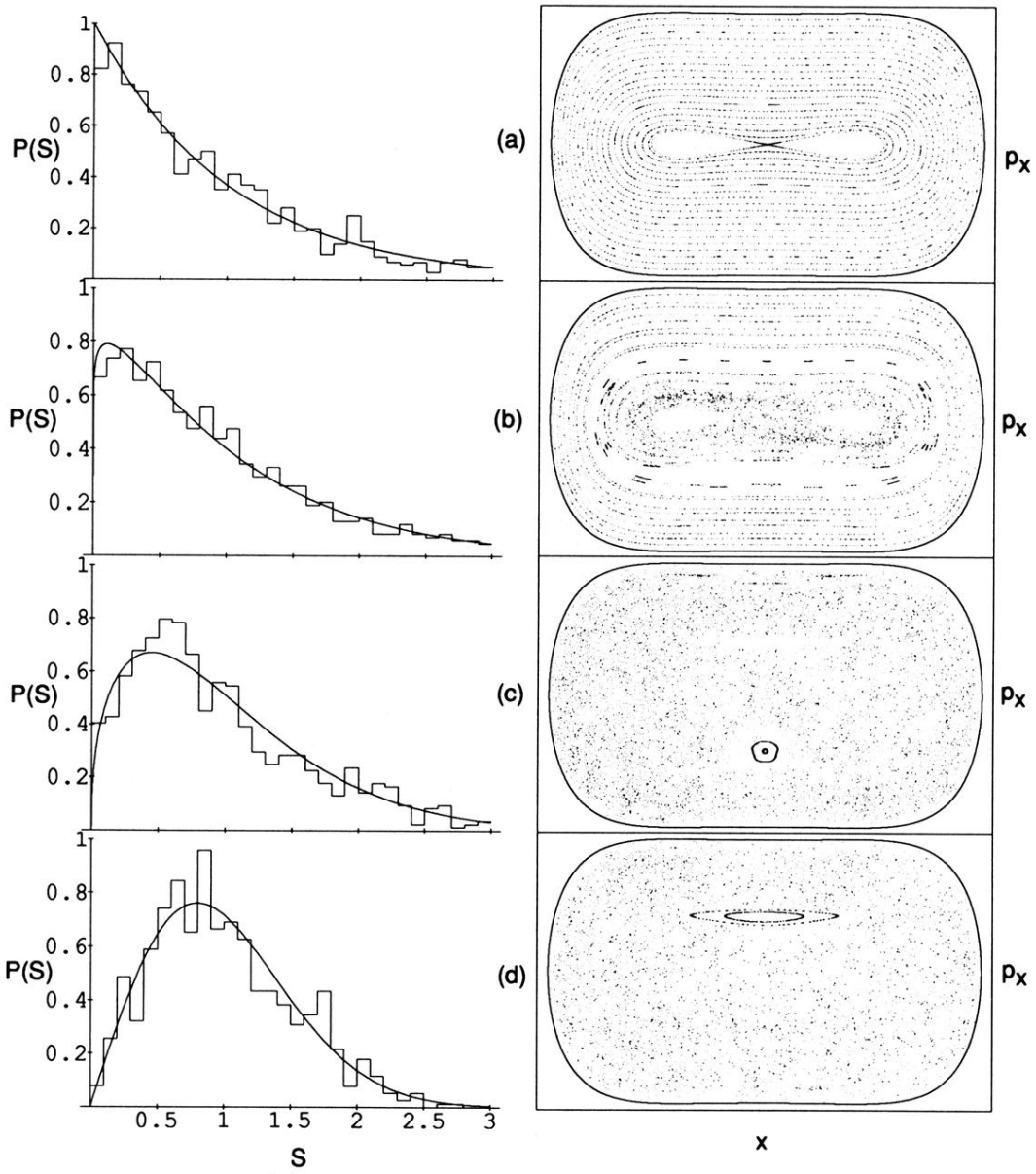

FIG. 2. Level spacing distributions $P(S)$ and the corresponding Poincaré cross sections of the model system with $g=0.2$ for (a) $\epsilon=0.0$, (b) $\epsilon=0.005$, (c) $\epsilon=0.04$, and (d) $\epsilon=0.10$. The cross sections are taken for $(y=0, p_y>0)$, where $\lambda=25$. The solid outlines represent the outermost boundary of the $\lambda=25$ energy surface as projected onto the (x,p_x) plane.